Spatial Power Amplifier Using a Passive and Active TEM Waveguide Concept

Mekki Belaid, *Student Member, IEEE*, and Ke Wu, *Fellow, IEEE*

***Abstract*—A new spatial power amplifier is presented in which power is spatially combined within a TEM waveguide using a low-loss transition array of E-plane integrated finlines to microstrip lines. The TEM-mode waveguide is implemented using a periodically patterned surface called a uniplanar compact electromagnetic bandgap (UC-EBG) structure. Our designed Ku-band back-to-back transition array demonstrates a maximum return loss of 17.5 dB and a maximum insertion loss of 0.65 dB. The TEM waveguide is found to have a 1-GHz bandwidth centered at 14.5 GHz. Tuning of the center frequency may be accomplished via an active UC-EBG structure that incorporates varactor diodes. The use of the UC-EBG surface allows more power cards to be inserted within the TEM waveguide since the amplifier cells saturate uniformly. The spatial power combiner is used to combine the output powers of 12 20-mW monolithic-microwave integrated-circuit amplifier chips. The designed power module yields an output power of 23.15 dBm and a combining efficiency of 86%. A comparison between the passive and active UC-EGB surfaces is experimentally demonstrated.**

***Index Terms*—Electromagnetic bandgap (EBG) structure, finline, power amplifier (PA), spatial power combiner, TEM waveguide, tunable device, varactor.**

I. Introduction

POWER amplifiers (PAs) are crucial in the design of wireless communication systems and, in particular, transmitter hardware. PAs can generally be made to have high-performance characteristics at low microwave frequencies, however, they are still limited in power and are difficult to design at higher microwave and millimeter-wave frequencies. This has stimulated a special interest in finding alternative solutions.

A well-justified potential technique is spatial power combining [1], for example, the tray-type of quasi-optical architecture. A remarkable advantage of using such an approach is that the insertion loss usually does not increase by increasing the number of amplifier elements or cells. This can be very attractive for the design of high-power systems in which a large number of low-power devices are combined. This is in fact a typical scenario at higher microwave and millimeter-wave frequencies for which a single-element high-power device may not be available or simply too expensive to use.

Manuscript received November 27, 2001. This work was supported by the Natural Sciences and Engineering Research Council of Canada.

The authors are with the Poly-Grames Research Center, Département de génie électrique et de génie informatique, École Polytechnique de Montréal, Montréal, QC, Canada H3C 3A7 (e-mail: wuke@grmes.polymtl.ca).

Digital Object Identifier 10.1109/TMTT.2003.808698

A number of approaches to solving this problem were proposed [2]–[5]. In [2]–[5], a broad-band spatial power combining technique using dense finline arrays was proposed and output powers ranging from 20 to 120 W were demonstrated at the X-band. This technique, however, is limited in the number of active devices that may be combined due to the nonuniform TE_{10} electric field profile across the waveguide. To increase the maximum number of power cards in the waveguide, a technique has been developed [6] in which an oversized combiner was designed to accommodate more cards. In this case, both the TE_{10} and TE_{20} modes propagate; however, by using a symmetric loading of the structure, modes of odd symmetry such as the TE_{20} mode can be effectively suppressed.

Recently, a periodically patterned surface called a photonic bandgap (PBG) or electromagnetic bandgap (EBG) structure has been useful in enhancing the performance of microwave circuits. A uniplanar compact electromagnetic bandgap (UC-EBG) structure was presented for various applications [7], [8]. In [9], a TEM waveguide using this periodic structure was developed. This structure realizes a magnetic surface in its stopband and is used to replace the two bilateral waveguide walls so as to satisfy a magnetic boundary condition. In this way, the TEM modal condition is satisfied in the rectangular waveguide, and a relatively uniform field distribution along the cross section can be obtained over a narrow bandwidth. This problem of bandwidth may impair the advantages of the proposed TEM waveguide solution.

The UC-EBG structure is in fact a class of planar frequency-selective surfaces (FSSs). Active FSS concepts were described earlier in [10]. In one case, active FSS elements incorporating p-i-n diodes were used to switch the frequency response from that of a reflecting structure to one of a transmitting structure. In another case, the FSS was printed on a ferrite substrate, and the application of a dc bias field to the ferrite allowed for the tuning of its resonant frequency by several gigahertz.

In this work, a novel spatial PA designed with both passive and active TEM waveguides is presented. In Section II, the characteristics and realization of both passive and active perfect magnetic conductors (PMCs) are presented. In Section III, the design of tapered finline arrays and, more importantly, the design of a new low-loss transition between finlines and microstrip lines is presented. This same transition can also be used to excite the nonconventional TEM waveguide. Section IV illustrates the fabrication and measurement aspects of the spatial waveguide PA and integrates the different components discussed in the previous sections.

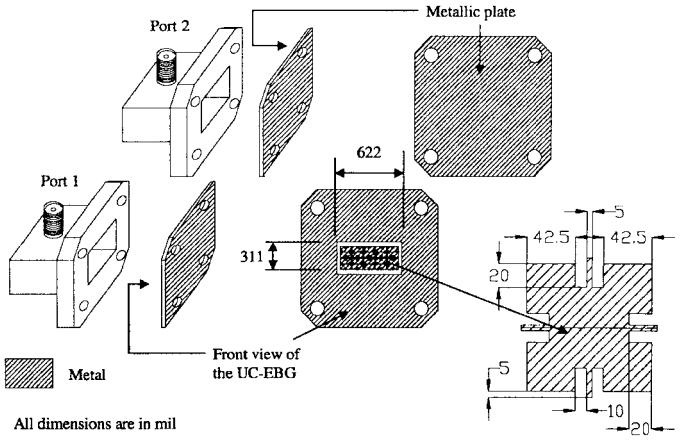

Fig. 1. Periodic pattern design of the UC-EBG and its experimental characterization techniques.

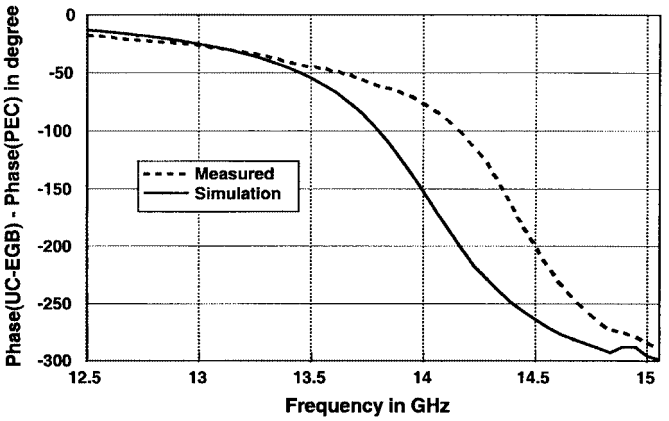

Fig. 2. Measured and simulated results of phase difference in the reflection coefficient between the EBG surface and a metallic plate for a planar wave incidence.

II. Design and Measurements of the Periodically Patterned Structure

A. Passive UC-EBG

Fig. 1 illustrates the UC-EBG surface and the measurement technique that was employed. This structure is a two-dimensional (2-D) periodic lattice patterned on a metallized dielectric substrate. The surface impedance of the proposed structure is frequency dependent and may be modeled as a distributed *LC* network with specific resonant frequencies (f_r). At these frequencies, the periodic loading becomes an open circuit and an equivalent magnetic surface is thus created. This phenomenon can be examined through experiment by measuring the reflection coefficient. The phase of the reflection coefficient of a PMC should exhibit a difference of 180° compared to that of a perfect electric conductor (PEC).

To verify this property, an intact copper sheet (PEC) and a UC-EBG surface (PMC), both fabricated on a conductor backed substrate (Duroid 6010) with a dielectric constant of 10.2 and a thickness of 25 mm, were utilized. Fig. 2 illustrates the difference in the angle of the reflection coefficient between the EGB and PEC surfaces. The measurements were performed with an Agilent HP8510 network analyzer. The analyzer was calibrated with a standard coaxial calibration kit. The procedure adopted to measure the phase difference between an electric and a magnetic surface is shown in Fig. 1. The two printed circuits are placed directly on the flanges of the WR62 waveguide to coaxial adapters. The reflection coefficients are measured at ports 1 and 2 (port 1 is the magnetic surface and port 2 is the electric surface). The network analyzer then computes the phase difference. As can be seen, a 180° phase difference occurs at approximately 14.4 GHz, indicating that a magnetic surface has successfully been realized. A theoretical simulation based on a commercial HFSS package is also illustrated in Fig. 2. It is in excellent agreement with that obtained experimentally. The discrepancy of approximately 3% might be the result of the perfect conductor assumption and dielectric consideration in the HFSS simulations.

Fig. 3 illustrates the transmission coefficient of a waveguide that incorporates UC-EBG surfaces at its bilateral sides. There are no particular transitions between the TE_{10} waveguide and the TEM waveguide. As shown in Fig. 3, the waveguide behaves as a stopband filter over a frequency band of approximately 1 GHz. It is thus necessary to design a transition to excite a TEM mode in the waveguide. This will be discussed in Section III.

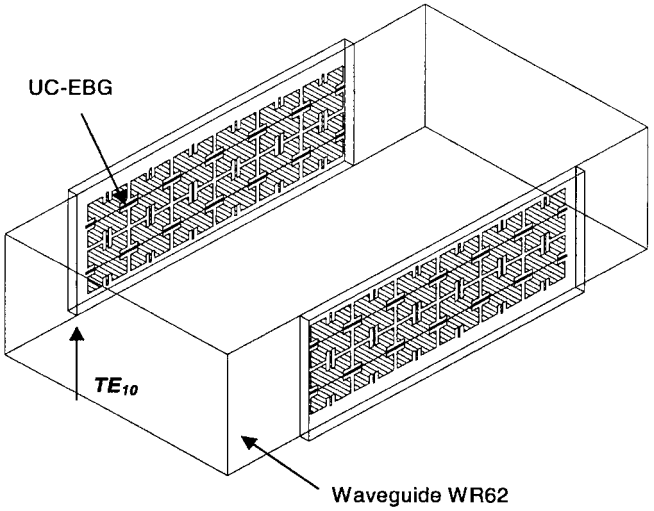

(a)

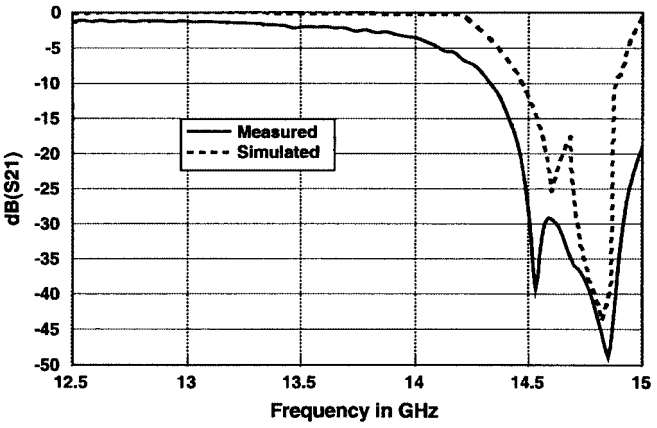

(b)

Fig. 3. Measured transmission coefficient S_{21} in the waveguide using the UC-EBG surface. (a) Setup for S_{21} measurement. (b) Measured and simulated results.

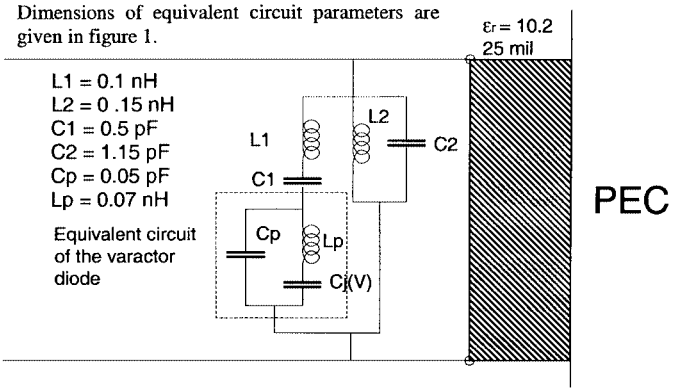

Fig. 4. Equivalent circuit for a varactor-based active periodic cell.

B. Active UC-EGB

The active UC-EBG consists of a large number of periodic cells embedded with active devices such as varactor or p-i-n diodes. In the present work, the varactor was chosen as the active element. Each diode in the array can be modeled by an equivalent electronic network in addition to the inherent impedance of the metal pattern of each unit cell. By assuming an infinite grid with a uniform plane wave normally incident upon the grid, the symmetry and periodicity of the structure allow us to replace the walls of the unit cell in the grid with electric and magnetic walls to form an equivalent unit-cell waveguide. Therefore, the analysis of the entire grid can be reduced to a simpler analysis of the equivalent unit-cell waveguide.

For a TEM incident wave with a vertically polarized electric field, the unit-cell waveguide has magnetic walls on both sides and electric walls on the top and bottom. The propagating modes in the unit-cell waveguide include a TEM mode and the evanescent modes coupled to (or generated by) currents flowing in the metal patterns. Note that the TE_{10} mode generates both longitudinal and nonlongitudinal currents while the current of the TEM mode has only a longitudinal component. This current discontinuity is responsible for the modal mismatch and the generation of higher order evanescent modes that are quickly attenuated within the waveguide. The current paths are limited in the unit cell by symmetry and cell topology. Therefore, the geometry of the cell is one of the critical issues in the design of a TEM waveguide that is poised to minimizing the effects of the other unwanted modes. A general rule is to guarantee a continuous longitudinal current flow while minimizing the flow of nonlongitudinal currents.

The equivalent unit-cell waveguide incorporating the varactor diodes can be represented by a simple transmission-line model. This model can be used to assess the performance of the entire grid as long as we know the equivalent circuit of the active device and the embedded impedance of the metal pattern. The equivalent circuit of the UC-EBG circuit proposed in [12] is showed in Fig. 4. To determine the equivalent circuit, we used a commercial software package HP-HFSS, a 3-D finite-element electromagnetic wave solver. Fig. 5 shows the structure to be simulated. Port 1 is the front port of the unit-cell waveguide and port 2, the driving point of the diode, is connected to a short section of a rectangular coaxial waveguide. The short section of this rectangular coaxial waveguide connected to the driving

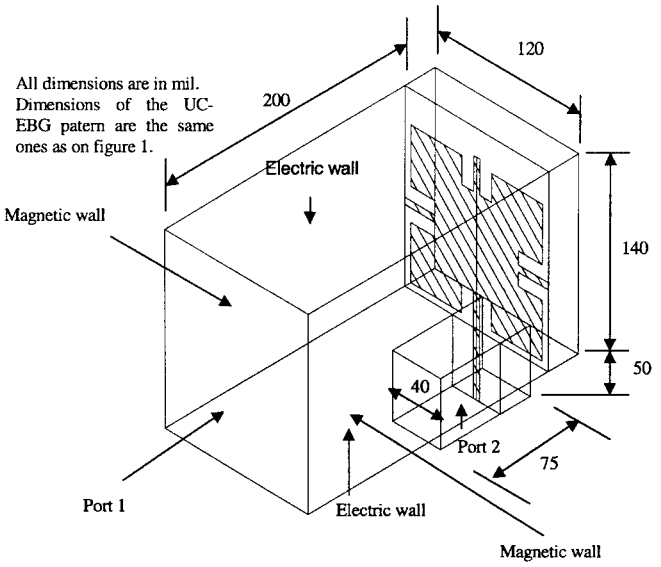

Fig. 5. The unit-cell waveguide used in HFSS simulations to extract the equivalent circuit.

point is well defined with a known propagation constant and waveguide impedance. Simulations over the frequency range of interest are carried out to calculate the S parameters. Postprocessing on the S parameters is required to remove the effects of the coaxial waveguide, namely, de-embedding the phase shift and renormalizing the S-parameter matrix.

The varactor diode used in our experiments is MA46580 from M/A-COM. The equivalent circuit of this diode is extracted using HP Integrated Circuit Characterization and Analysis Program (IC-CAP). The diodes were connected in the y direction and the bias lines were introduced perpendicular to the electric field. Fig. 6(a) shows the experimental setup of the wave scattering measurements made on the active UC-EGB surface. In Fig. 6(b), the measured and simulated resonant frequency (f_r) of the active surface is plotted against the reverse bias voltage applied to the varactor diode. Simulated results based on the model show a good agreement with the measurements. It is apparent that the frequency of resonance can be tuned from 14.55 to 16.56 GHz.

III. Design of Spatial Power Combiner in a Waveguide

The topology of the broad-band spatial power combiner is based on the work of Cheng *et al.* [2]. As illustrated in Fig. 7, this combiner consists of a 2-D array of finline antennas in the form of tapered slotline sections with transition to microstrip lines. These cards are mounted onto a thin metal test fixture for mechanical stability and heat removal, and then inserted in a standard Ku-band waveguide. The finline antenna sections serve as impedance-matching transformers between the microstrip line and the TE waveguide. Our design is based on the theory of small reflections as well as the analytical results of Klopfenstein's taper,as detailed in [11]. HFSS was used to analyze the finline array structure to obtain the relation between the physical dimensions of the structure and the input impedance and propagation constant. The finline was fabricated on a Duroïd substrate with a dielectric constant of 2.22 and a thickness of 10 mm. The

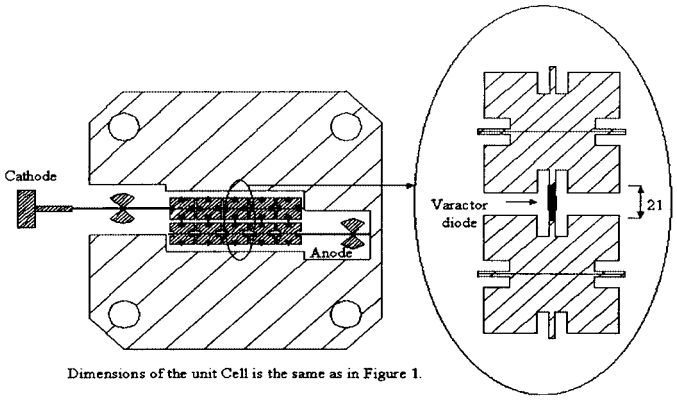

(a)

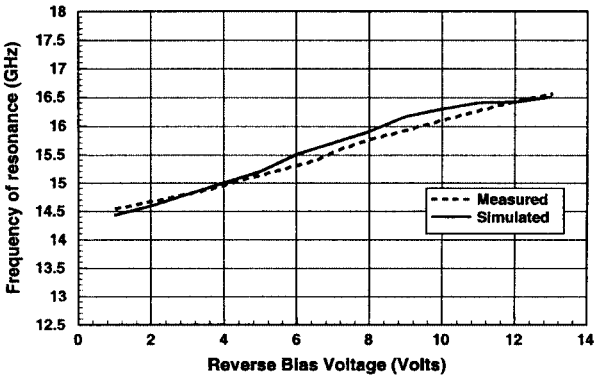

(b)

Fig. 6. Investigation of tunable UC-EBG surface. (a) Setup for the reflection coefficient measurement. (b) Measured and simulated frequency of resonance of the active UC-EBG surface.

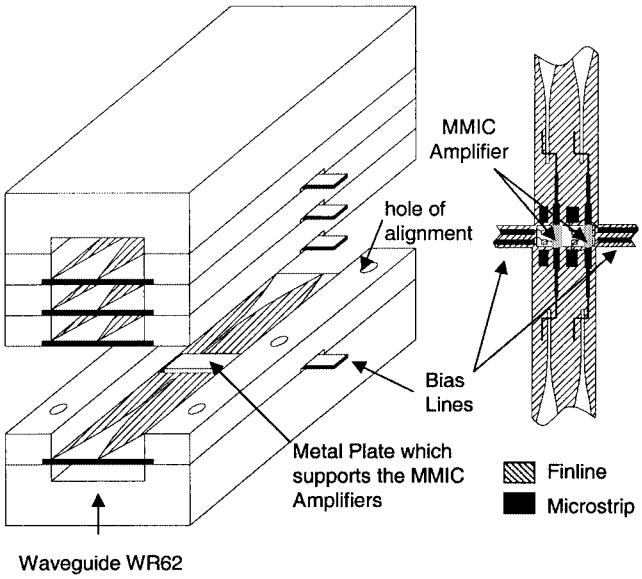

Fig. 7. Tray-type topology of the spatial power combiner housing multiple cards.

design of the impedance-matching network between the finline and the microstrip line was inspired by the work carried out on the transition between microstrip lines and slotlines. The transition considered here is sketched in Fig. 8. Due to our current fabrication restriction, the smallest gap that we can obtain for

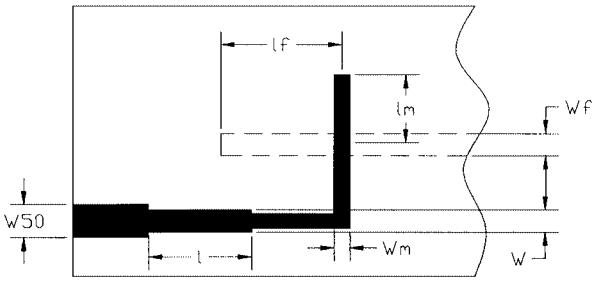

Fig. 8. Transition design between the finline and microstrip line.

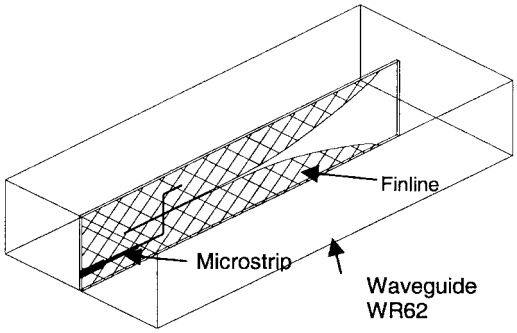

Fig. 9. TEM-mode launcher for experimental characterization of the TEM-mode waveguide.

the finline is 6 mm. This corresponds to a line with a characteristic impedance of approximately 117 Ω. The dimensions were chosen for a center frequency of about 15.25 GHz. The microstrip transition line width and stub length were respectively selected as $Wm = 5.7$ mm and $lm = 150.9$ mm to obtain a characteristic impedance of 116 Ω. For the finline, the width is $Wf = 6$ mm and the stub length is $Lf = 172.8$ mm. To transform the impedance Zm to 50 Ω, a quarter-wave transformer with characteristic impedance of 76.2 Ω was used. The dimensions of this line are $W = 14.9$ mm and $l = 143.1$ m. The test circuit is schematically illustrated in Fig. 9. The measured return and insertion losses of the back-to-back transitions are shown in Fig. 10. The return loss is better than 17.5 dB for the entire waveguide band. The maximum insertion loss is 0.65 dB. It is worth mentioning that theoretically there is no upper limit for the bandwidth of the gradual taper line. The bandwidth is actually limited by the transition between the microstrip line and the finline and by the choice of waveguide.

IV. Measurements of the Proposed Amplifier

A. Passive TEM Waveguide

To effectively launch the TEM mode in the waveguide, the same transition between the finline and microstrip was used. This avoids the use of a special transition between the TE_{10} waveguide and the TEM waveguide. The topology of the finline is recalculated in this case to account for the new impedance profile of the TEM waveguide. A broad-band response with a low return loss (> 16 dB) has been obtained.

To obtain a better understanding of the effects of replacing the bilateral walls of the waveguide with the UC-EBG surfaces, two designs were realized. The first design used six power cards inside the waveguide without the UC-EBG surfaces, whereas

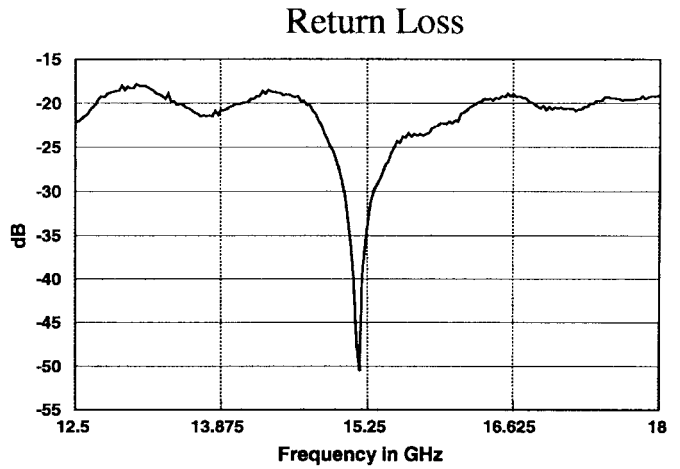

(a)

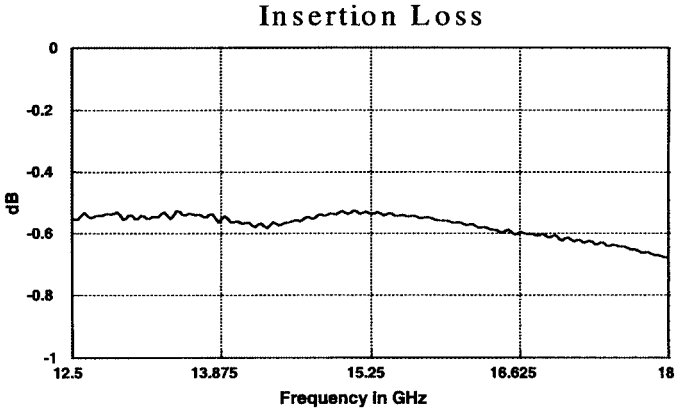

(b)

Fig. 10. Measured results of the transition between finline and microstrip line. (a) Return loss. (b) Insertion loss.

the second utilized the UC-EBG surfaces to create the TEM waveguide. Each card contains two low-cost MMIC (GaAstek-ITT3502D) amplifier cells, each producing an output power of 20 mW. The distance between the cards was set at 80 mm. Fig. 11 displays the measured results of the output power versus the input power. This measurement was taken at 14.75 GHz, within the operable range of the UC-EBG surface. It is noticed that including the UC-EBG surfaces increased the output power by 1.5 dBm. This can easily be explained by the fact that, due to the more uniform distribution of the field with the TEM waveguide, the amplifier cells on the power cards compress or saturated almost simultaneously, whereas in the TE waveguide the amplifier cells that are more centrally located start to compress before the other cells.

The efficiency of the whole power combining system is equal to the efficiency of the amplifier cell multiplied by the loss of the passive combiner when the gain of the amplifier cell becomes very large. The combiner loss can be calculated by the following equation using S-parameters of a through line measurement:

$$LF \approx \sqrt{\frac{|S_{21}|^2}{1-|S_{11}|^2}}. \tag{1}$$

Our average combining loss of 0.65 dB indicates that a combining efficiency of better than 86% can readily be achieved.

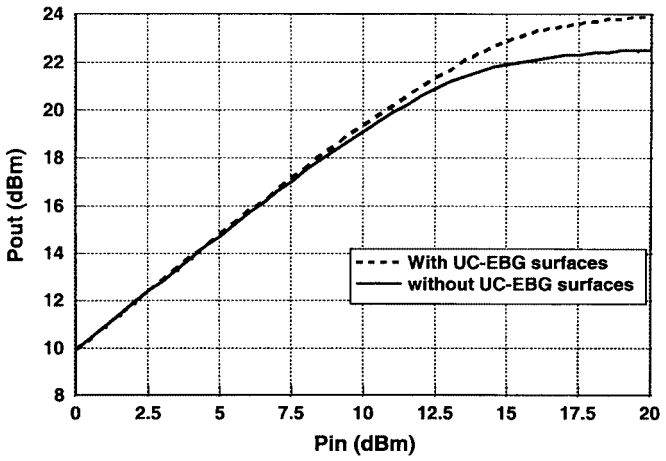

Fig. 11. Measured output power with and without UC-EBG surfaces at 14.75 GHz.

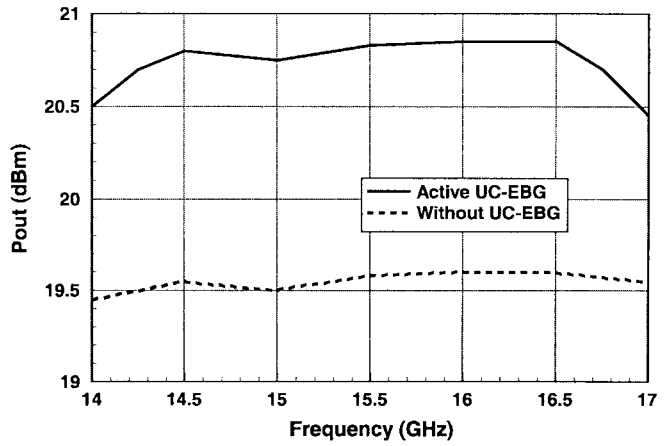

Fig. 12. Measured output power of a waveguide amplifier with and without active UC-EBG surfaces.

B. Active TEM Waveguide

The same passive structure was used to build the active TEM waveguide amplifier. The difference is that the UC-EBG surface incorporates the electronically tunable varactor diodes. Fig. 12 shows a comparison between the measured output power of the active UC-EBG amplifier and the same amplifier without the UC-EBG surfaces. An increase in the output power of 1.0–1.25 dBm is observed over the frequency range of 14–17 GHz. The voltage was tuned for each measurement.

The varactor diodes introduce an additional loss of 0.25 dB that effectively reduces the combining efficiency to 82.2%; however, the effective bandwidth is increased by 2 GHz.

V. Conclusion

This work has demonstrated the use of passive and active TEM waveguides in the design of an improved spatial power combiner. This novel design incorporates a UC-EBG surface, to effectively create the TEM waveguide, and improves the output power by 1.5 dBm over a 1-GHz bandwidth when the MMIC amplifiers are driven close to their compression points. An active UC-EBG surface may be used to increase the bandwidth to 3 GHz; however, the additional loss introduced by the varactor diodes reduces the output power by 0.25 dB for an improvement

of 1.25 dBm. This increase in the output power is significant in the higher microwave and millimeter-wave frequencies where this technique is often employed.

REFERENCES

[1] M. A. Gouker, "Spatial power combining," in *Active and Quasi-Optical Arrays for Solid-State Power Combining*, R. A. York and Z. B. Popovic, Eds. New York: Wiley, 1997.

[2] N. S. Cheng, A. Alexanian, M. G. Case, and R. A. York, "20 watt spatial power combiner in waveguide," in *IEEE MTT-S Int. Microwave Symp. Dig.*, Baltimore, MD, June 1998, pp. 1457–1460.

[3] ——, "40-W CW broad-band spatial power combiner using dense finline arrays," *IEEE Trans. Microwave Theory Tech.*, vol. 47, pp. 1070–1076, July 1999.

[4] N. S. Cheng, T. P. Dao, M. G. Case, D. B. Rensch, and R. A. York, "A 60-watt X-band spatially combined solid state amplifier," in *IEEE MTT-S Int. Microwave Symp. Dig.*, Anaheim, CA, June 1999, pp. 539–542.

[5] N. S. Cheng, P. Jia, D. B. Rensch, and R. A. York, "A 120-watt X-band spatially combined solid state amplifier," *IEEE Trans. Microwave Theory Tech.*, vol. 47, pp. 2557–2561, Dec. 1999.

[6] L. Y. V. Chen and R. A. York, "Development of K-band spatial combiner using active array modules in an oversized rectangular waveguide," in *IEEE MTT-S Int. Microwave Symp. Dig.*, Boston, MA, June 2000, pp. 821–824.

[7] M. Kim, J. B. Hacker, A. L. Sailer, S. Kim, D. Sievenpiper, and J. A. Higgins, "A rectangular TEM waveguide with photonic crystal walls for excitation of quasioptical amplifiers," in *IEEE MTT-S Int. Microwave Symp. Dig.*, Anaheim, CA, June 1999, pp. 543–546.

[8] Y. Qian and T. Itoh, "Planar periodic structures for microwave and millimeter wave circuit applications," in *IEEE MTT-S Int. Microwave Symp. Dig.*, Anaheim, CA, June 1999, pp. 1533–1536.

[9] F. R. Yang, K. P. Ma, Y. Qian, and T. Itoh, "A novel TEM waveguide using uniplanar compact photonic-bandgap (UC-PGB) structure," *IEEE Trans. Microwave Theory Tech.*, vol. 47, pp. 2092–2097, Nov. 1999.

[10] T. K. Chang, R. J. Langley, and E. A. Parker, "Active frequency-selective surfaces," *Proc. Inst. Elect. Eng.*, pt. H, vol. 143, no. 1, Feb. 1996.

[11] R. W. Klopfenstein, "A transmission-line taper of improved design," *Proc. IRE*, vol. 442, pp. 31–35, Jan. 1956.

[12] J. A. Arnaud and F. A. Pelow, "Resonant-grid quasioptical diplexers," *Bell Syst. Tech. J.*, vol. 54, no. 2, pp. 263–283, Feb. 1975.

Mekki Belaid (S'96) received the B.Eng. degree in electrical engineering and M.A.Sc. degree from the École Polytechnique de Montréal, Montreal, QC, Canada, in 1996 and 1998, respectively, and is currently working toward the Ph.D. degree at the École Polytechnique de Montréal.

Ke Wu (M'87–SM'92–F'01) was born in Liyang, Jiangsu Province, China. He received the B.Sc. degree in radio engineering (with distinction) from the Nanjing Institute of Technology (now Southeast University), Nanjing, China, in 1982, and the D.E.A. and Ph.D. degrees in optics, optoelectronics, and microwave engineering (with distinction) from the Institut National Polytechnique de Grenoble (INPG), Grenoble, France, in 1984 and 1987, respectively.

He conducted research in the Laboratoire d'Electromagnetisme, Microondes et Optoelectronics (LEMO), Grenoble, France, prior to joining the Department of Electrical and Computer Engineering, University of Victoria, Victoria, BC, Canada. He subsequently joined the Department of Electrical and Computer Engineering, Ecole Polytechnique de Montréal (Faculty of Engineering, University of Montréal) as an Assistant Professor, and is currently a Full Professor and Tier-I Canada Research Chair in Radio-Frequency and Millimeter-Wave Engineering. He has been a Visiting or Guest Professor at Telecom-Paris, Paris, France, and INP-Grenoble, Grenoble, France, the City University of Hong Kong, the Swiss Federal Institute of Technology (ETH-Zurich), Zurich, Switzerland, the National University of Singapore, Singapore, the University of Ulm, Ulm, Germany, as well as many short-term visiting professorships with other universities. He also holds an honorary visiting professorship at the Southeast University, Nanjing, China, and an honorary professorship at the Nanjing University of Science and Technology, Nanjing, China. He has been the Head of the FCAR Research Group of Quebec on RF and microwave electronics, the Director of the Poly-Grames Research Center, as well as the Founding Director of the newly developed Canadian Facility for Advanced Millimeter-Wave Engineering (FAME). He has authored or coauthored over 340 referred papers, and also several book chapters. His current research interests involve hybrid/monolithic planar and nonplanar integration techniques, active and passive circuits, antenna arrays, advanced field-theory-based computer-aided design (CAD) and modeling techniques, and development of low-cost RF and millimeter-wave transceivers. He is also interested in the modeling and design of microwave photonic circuits and systems. He serves on the Editorial Board of *Microwave and Optical Technology Letters* and Wiley's *Encyclopedia of RF and Microwave Engineering*.

Dr. Wu is a member of the Electromagnetics Academy, the Sigma Xi Honorary Society of the URSI. He has held many positions in and has served on various international committees, including the vice chairperson of the Technical Program Committee (TPC) for the 1997 Asia–Pacific Microwave Conference, the general co-chair of the 1999 and 2000 SPIE International Symposium on Terahertz and Gigahertz Electronics and Photonics, and the general chair of 8th International Microwave and Optical Technology (ISMOT'2001). He has served on the Editorial or Review Boards of various technical journals, including the IEEE TRANSACTIONS ON MICROWAVE THEORY AND TECHNIQUES, the IEEE TRANSACTIONS ON ANTENNAS AND PROPAGATION, and the IEEE MICROWAVE AND GUIDED WAVE LETTERS. He served on the 1996 IEEE Admission and Advancement (A&A) Committee, the Steering Committee for the 1997 joint IEEE Antennas and Propagation Society (IEEE AP-S)/URSI International Symposium. He has also served as a TPC member for the IEEE Microwave Theory and Techniques Society (IEEE MTT-S) International Microwave Symposium. He was elected into the Board of Directors of the Canadian Institute for Telecommunication Research (CITR). He served on the Technical Advisory Board of Lumenon Lightwave Technology Inc. He is currently the chair of the joint IEEE chapters of MTT-S/AP-S/LEOS in Montréal, QC, Canada. He was the recipient of a URSI Young Scientist Award, the Institute of Electrical Engineers (IEE), U.K., Oliver Lodge Premium Award, the Asia–Pacific Microwave Prize Award, the University Research Award "Prix Poly 1873 pour l'Excellence en Recherche" presented by the Ecole Polytechnique de Montréal on the occasion of its 125th anniversary, and the Urgel-Archambault Prize (the highest honor) in the field of physical sciences, mathematics, and engineering from the French–Canadian Association for the Advancement of Science (ACFAS). In 2002, he was the first recipient of the IEEE MTT-S Outstanding Young Engineer Award. He was inducted as a Fellow of the Canadian Academy of Engineering (CAE) in 2002.